



The effects of starting microstructure on the results of double intercritical annealing process of 0.107%C-2.39%Mn-0.453%Si dual phase steel

Wichayut CHUMOUNG¹, and Nithi SAENARJHAN^{1,*}

¹ Department of Metallurgical Engineering, Faculty of Engineering, Chulalongkorn University, Bangkok, 10330, Thailand

*Corresponding author e-mail: Nithi.S@chula.ac.th

Received date:

17 May 2024

Revised date:

18 October 2024

Accepted date:

27 December 2024

Keywords:

Dual phase steel;
Heat treatment;
Intercritical annealing;
Mechanical properties

Abstract

This study investigates and compares the effects of the starting microstructure on the double intercritical annealing (DIA) process on the microstructure and mechanical properties of 0.11%C-2.39%Mn-0.45%Si dual phase steel. The specimens were austenitized, followed by water quenching (WQ) or air cooling (AC), then DIA at 730°C. For the WQ method, high cooling rate results in the formation of a high strength martensitic structure. Conversely, AC method yields a moderate cooling rate, forming a bainitic structure. After single intercritical annealing (SIA), the microstructure transformed into ferrite and martensite. WQ method specimens contain high stress concentration, leading to earlier recrystallization compared to the AC method resulting in a higher amount of martensite and a larger ferrite grain area. In contrast, the AC method results in more homogeneous structure, thus it shows lower strength with higher ductility compared to the WQ method. After DIA, the WQ method has a higher strength than the AC method, with similar ductility. This is because the morphology of the martensite in WQ730SIA is thin and sharp needle dispersed irregularly in matrix which has a higher stress concentration than AC730SIA which has short and rounded martensite dispersed regularly in ferrite matrix. However, regardless of slightly higher mechanical properties, the WQ method causes the risk of the workpiece breaking during first water quenching, therefore, the AC method provides a better heat treatment option.

1. Introduction

Dual phase (DP) steels are a kind of advanced high strength steels (AHSS) [1] which generally, is low carbon steels (0.05 wt% C to 0.25 wt% C) [2]. The microstructure consists of martensite as the hard phase and ferrite as the ductile phase. Its distinctive features include low yield strength facilitating ease of shaping, absence of yield point phenomenon, high strain hardening rate, and good weldability. Compared to high strength low alloy steels (HSLA) with similar tensile strength, DP steels have lower yield strength, higher ductility and additionally, increased strength through work hardening [3].

There has been extensive researches on the need to increase tensile strength without sacrificing the ductility of DP steel [4-10]. This is achieved through the modification of the microstructure via the heat treatment process [4-6]. There are 2 main processes involved for the heat treatment of DP steels, austenitizing and intercritical annealing. Heat treatments are the most straight forward methods to enhance the properties of low alloy steel by adjusting various parameters such as temperature, time [7], and cooling rate [8]. These significantly influence the mechanical properties and determining factors such as the microstructure, phase distribution of martensite [9], and the size of ferrite grains [2].

The intercritical annealing is crucial for the production of DP steel because it significantly influences the proportion of martensite

phases [10]. The controlled adjustment of martensite content during intercritical annealing results in varying tensile strength ranging from 400 MPa to 1000 MPa, making the DP steel suitable for applications in automotive and other industries [11,12].

Furthermore, it was observed that hot or cold deformation has an impact on the size and distribution of martensite in the DP steel, affecting the refinement of grains [13]. For example, post-intercritical annealing cold-rolling promotes ultra-fine grains (UFG) and deformation-induced ferrite transformation (DIFT) [14]. However, these techniques are primarily derived from sacrificing formability upfront, such as through extensive rolling or complex and expensive deformation paths [4,15]. Thus, this is not very practical for the production of DP steels. From the study [4], repeating the intercritical annealing cycle results in repeated recrystallization, leading to grain refinement, increased yield, and tensile strength. Meanwhile, uniform ductility and overall elongation are likely to experience an insignificant impact [4,6,11].

Until recently, the evolution of the microstructure from repeat intercritical annealing for grain refinement has received limited attention. Hence, it serves as the motivation for this research to investigate the impact of the initial microstructure on the outcomes of double intercritical annealing. This research studies the microstructure and mechanical properties. On the effects of different initial microstructures after double intercritical annealing of 0.107%C-2.39%Mn-0.453%Si dual phase steel.

2. Experimental

2.1 Materials and specimen preparation

Dual phase steel used in this study has a chemical composition as shown in Table 1. The specimen was cold rolled to a thickness of 1.4 mm, then cut into tensile test specimens according to ASTM E8 standard as shown in Figure 1.

2.2 Heat treatment

To choose the austenitizing temperature and the intercritical annealing temperature, calculations were performed for A1 and A3 temperatures based on the chemical composition using Equation (1-4) [16].

Hougardy;

$$A1 = 739 - 22C - 7Mn + 2Si + 14Cr + 13Mo - 13Ni \quad (1)$$

Trzaska;

$$A1 = 739 - 22.8C - 6.8Mn + 18.2Si + 11.7Cr - 15Ni - 6.4Mo - 5V - 28Cu \quad (2)$$

Hougardy;

$$A3 = 902 - 255C - 11Mn + 19Si - 5Cr + 13Mo - 20Ni + 55V \quad (3)$$

Trzaska;

$$A3 = 937.3 - 224.5C - 17Mn + 34Si - 14Ni + 21.6Mo + 41.8V - 20Cu \quad (4)$$

Two different equations were used to reduce the uncertainty of the A1 and A3 values based on the chemical composition. The calculated values for A1 from Equation (1-2) are 721°C and 728°C, respectively. Meanwhile, the calculated values for A3 from Equation (3-4) are 857°C and 887°C, respectively.

To obtain a fully austenitic structure, it is necessary to use a temperature higher than A3 by approximately 50°C and avoid excessively high temperatures as the austenite grain size increases with increasing temperature thus, temperature of 950°C was chosen. The intercritical annealing temperature, set between A1 and A3, was selected at 730°C.

Figure 2 shows the heat treatment process involved in heating the workpiece to 950°C for 10 min, followed by water quenching or air cooling. Subsequently, intercritical annealing was performed

twice at 730°C for 3 min, with water quenching as cooling method. Hereafter, the specimens are named regarding to their heat treatment condition for example the water quenched specimen, intercritical annealed once at 730°C is called "WQ730SIA". There are six conditions total: WQ950, AC950, WQ730SIA, WQ730DIA, AC730SIA, and AC730DIA (Table 2).

2.3 Tensile testing

In total, 6 conditions (Table 2) were tested for tensile properties at room temperature. During the elastic deformation, the specimens were pulled at a rate of 0.008 mm·s⁻¹, then, as the plastic deformation started, the speed was increased to 0.16 mm·s⁻¹. The tests were conducted three times for each specimen condition.

2.4 Microstructure characterization

Small piece of the tensile test specimens was cut from the grip section to observe the microstructure. The specimens were then grounded using sandpaper from 80 grit to 2000 grit, followed by polishing with 1 μm and 9 μm diamond powder then etched with nital solution 2%vol.

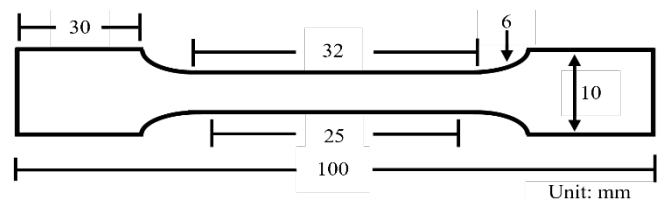


Figure 1. Schematic drawing of subsize tensile specimen (ASTM E8 standard).

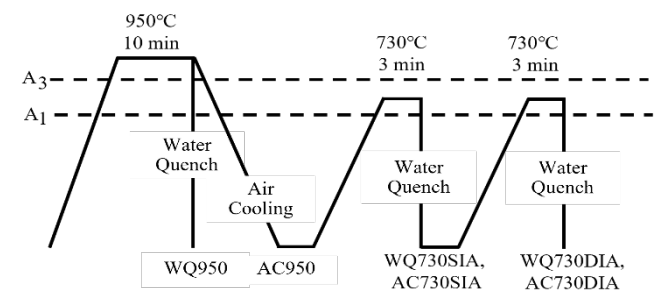


Figure 2. Heat treatment profile used in this study.

Table 1. Chemical composition of DP780 steel used in this study.

Chemical composition (wt%)							
C	Mn	Si	Cr	Mo	Ni	Cu	V
0.107	2.39	0.453	0.023	0.0072	0.021	0.014	0.0015

Table 2. Tensile test specimen's heat treatment conditions.

Specimen conditions	
Name	Heat treatment condition
AC950	950°C, 10 min + AC
AC730SIA	950°C, 10 min + WQ + 730°C, 3 min
AC730DIA	950°C, 10 min + WQ + 730°C, 3 min + 730°C, 3 min
WQ950	950°C, 10 min + WQ
WQ730SIA	950°C, 10 min + AC + 730°C, 3 min
WQ730DIA	950°C, 10 min + AC + 730°C, 3 min + 730°C, 3 min

An optical microscope (OM), was employed to examine the microstructure along the rolling direction. The average grain area of ferrite along with the fraction of martensite area were measured using ImageJ software.

Subsequently, a scanning electron microscope (SEM), JEOL JSM-6610LV, was utilized for detailed analysis of the microstructure. Energy Dispersive Spectroscopy (EDS) was also employed in line scan mode to identify the elemental distribution of each phase.

3. Results and discussion

3.1 Microstructure

The specimens, which were austenitized then subjected to the AC or WQ method, resulting in different microstructure (Figure 3). AC method leads to a bainitic initial microstructure as shown in Figure 3(a,c) due to the effect of manganese which delays the phase transformation [17]. On the other hand, WQ method which has a higher cooling rate results in a fully martensitic structure with a high stress concentration and a large amount of dislocation (Figure 3(b,d)) [18].

After SIA (Figure 4), Both AC (Figure 4(a,b)) and WQ (Figure 4(c,d)) methods the microstructure consists of ferrite and martensite distributed throughout every workpiece. The shape of ferrite was found in 2 types: granular ferrite and lath ferrite. During the intercritical annealing lath ferrite with needle-like shape was formed by the reversion of lath martensite or bainite while granular ferrite was formed at grain boundaries due to recrystallization [6]. Additionally, silicon also helps in the formation of granular ferrite [19].

Microstructure of the AC730SIA and WQ730SIA specimens are shown in Figure 4(a,b) and Figure 4(c,d), respectively. More lath ferrite was observed in the center compared to near surface area in both

specimens however, granular ferrite is the major type found near surface area. Moreover, the AC730SIA has more lath ferrite than the WQ730SIA, while the WQ730SIA has a larger number of granular ferrite. The morphology of martensite in the AC730SIA was short and rounded dispersed regularly in ferrite matrix. On the other hand, martensite in the WQ730SIA appears as thin and sharp needle dispersed irregularly throughout the microstructure. Therefore, the microstructures of AC730SIA and WQ730SIA specimens show different characteristics, as result from dissimilar initial microstructure.

Due to the difference in stress concentration resulting from different cooling methods, the recrystallization process progresses differently [20]. The WQ730SIA with higher stress concentration causes the recrystallization temperature to be lower (easier to recrystallize), and resulting in a larger number of granular ferrite. Meanwhile, the AC730SIA specimen has a lower stress concentration and therefore shows lesser number of granular ferrite. However, the short annealing time, compared to other research studies [12,21], was not enough for recrystallization to finish in all areas, especially in the central area [22]. Thus, the specimens demonstrate unevenness microstructure throughout the entire area.

After DIA, AC730DIA exhibits a smaller size of martensite, granular ferrite, and lath ferrite, resulting in a higher quantity and more uniform distribution as shown in Figure 5(a,b). The similarity in the phase morphology between the surface and center area indicates improved homogeneity after DIA. Similar behavior was also observed in WQ730DIA. However, for WQ730DIA (Figure 5(c,d)). There is still a noticeable difference between the near surface and the center area, as martensite appears to disperse irregularly, similar to WQ730SIA. Therefore, this suggests that the uniformity of WQ730DIA is less than that of AC730DIA.

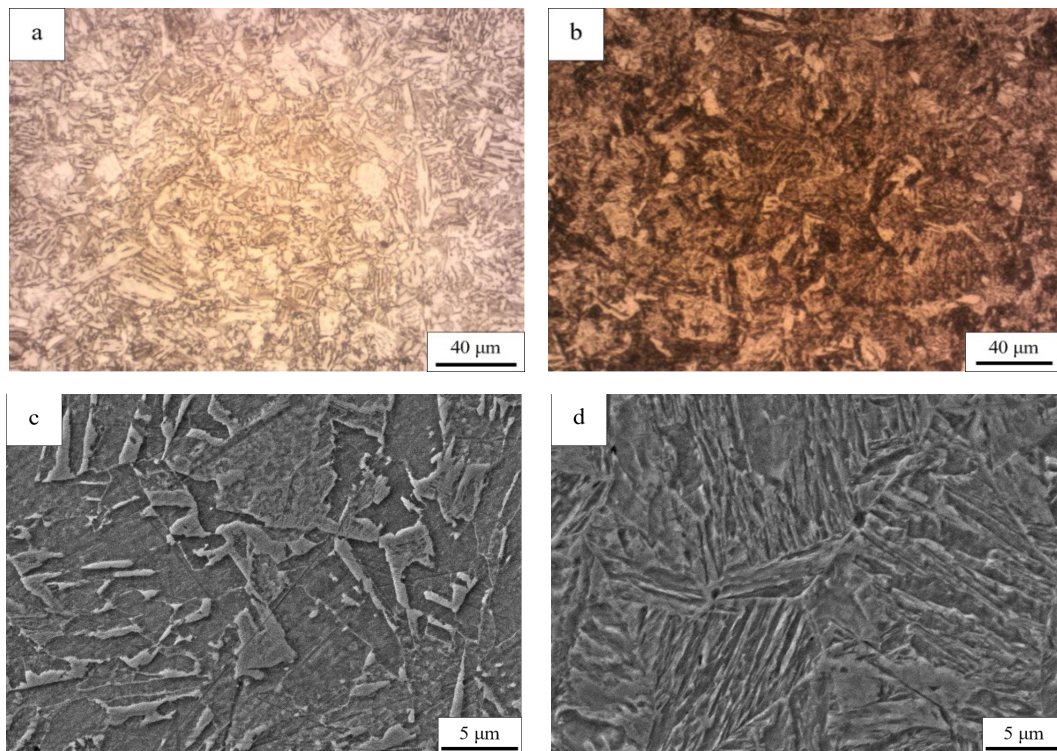


Figure 3. Microstructure after austenitized of (a,c) AC950 and (b,d) WQ950 [6] taken by (a,b) OM and (c,d) SEM [6].

Using grain ferrite area as a representation of grain ferrite size of samples with various heat treatment conditions, as shown in Table 3. This shows that all samples have an average ferrite grain area not exceeding $100 \mu\text{m}^2$. After SIA, WQ730SIA has a larger ferrite grain size than AC730SIA because water quenching produces higher stress concentration than air cooling [20]. This causes WQ730SIA specimen to undergo a phase transformation to austenite and ferrite phases and growth faster [22,23] than AC730SIA. Furthermore, the transformation is not uniform in both AC730SIA and WQ730SIA, due to uneven heating between near surface and center areas [22,23], as the heat experiences near surface area is longer than the center area. As a result, after water quenching, the near surface area has a larger ferrite grain size compared to the center area.

After DIA, the ferrite grain size decreased however, the WQ730DIA (Figure 5(c,d)) still has a larger ferrite grain size than the AC730DIA (Figure 5(a,b)), as the microstructure of WQ730DIA consists of more granular ferrite which has a large area and less amount of lath ferrite compared to the AC730DIA. In addition, it is interesting to note that the ferrite grain size measurement has a very high deviation in all heat treatment conditions. This refers to the difference in ferrite shapes, granular and lath, which show a significant different in ferrite grain size.

The martensite fraction is shown in Figure 6. WQ730SIA specimen has a slightly higher amount of martensite than AC730SIA due to the fully martensitic structure before SIA however, the difference is relatively low and insignificant. During SIA recrystallization occurs in WQ730SIA before the AC730SIA as a result of higher stress concentration [20]. Nevertheless, since the intercritical annealing time is short, fully recrystallization was not complete especially in the center areas. Therefore, martensite was not fully transformed in many areas of both specimens and still present after SIA. This results in the slightly higher martensite fraction of WQ730SIA and also the diversity of martensite fraction in both specimens depending on areas.

After DIA, both AC730DIA and WQ730DIA specimens have almost similar martensite fraction, approximately 60%, which are slightly lower than SIA condition. The diversity of martensite fraction between near surface and the center area stay close to after SIA and the difference is still observable. This indicates that the short time intercritical temperature annealing at 730°C is not enough to make the uniform microstructure [24] even after DIA. This discrepancy is due to insufficient energy resulting from the short annealing time and low temperature thus, preventing complete martensite recrystallization. As a result, the microstructure in the center area is not fully resemble that near surface area.

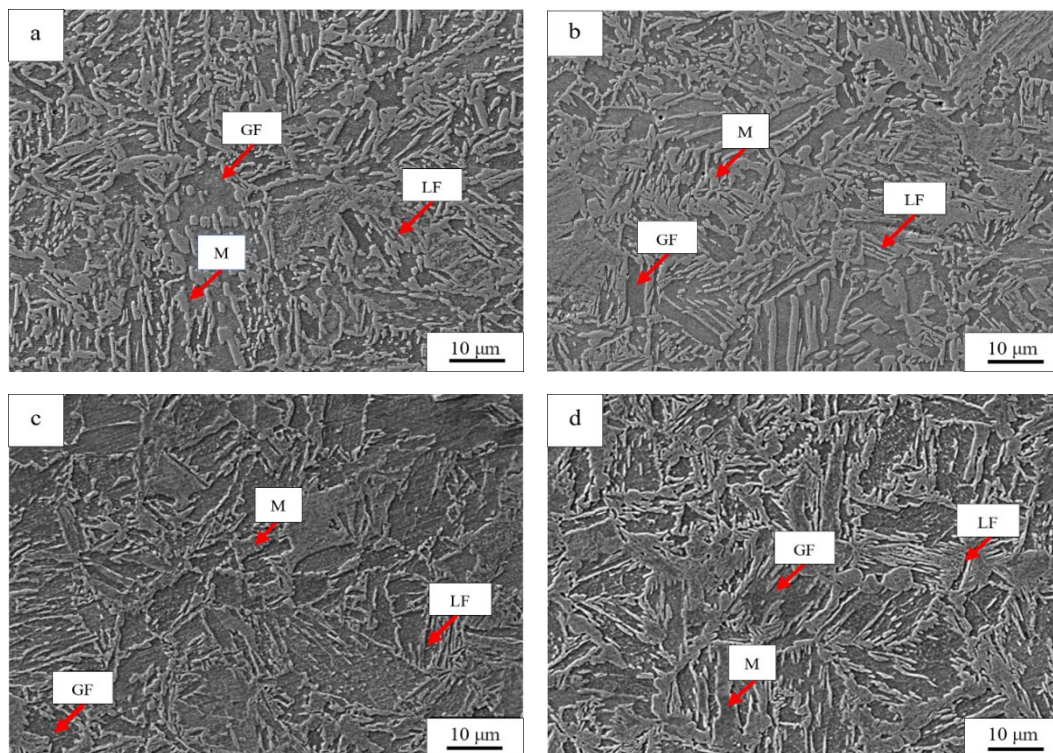


Figure 4. SEM micrographs of (a,b) AC730SIA and (c,d) WQ730SIA [6], (a,c) near surface area and (b,d) at center area. LF: Lath ferrite, GF: Granular ferrite, M: Martensite.

Table 3. Average ferrite grain area of specimens with various heat treatment conditions.

Specimen	Surface [μm^2]	Center [μm^2]	Overall [μm^2]
AC730SIA	79.96 ± 49.12	48.83 ± 33.65	64.39 ± 20.16
AC730DIA	61.95 ± 38.37	43.57 ± 25.87	52.76 ± 33.99
WQ730SIA [6]	96.63 ± 80.08	58.15 ± 55.58	77.39 ± 71.46
WQ730DIA [6]	66.22 ± 51.55	54.36 ± 48.07	60.29 ± 50.11

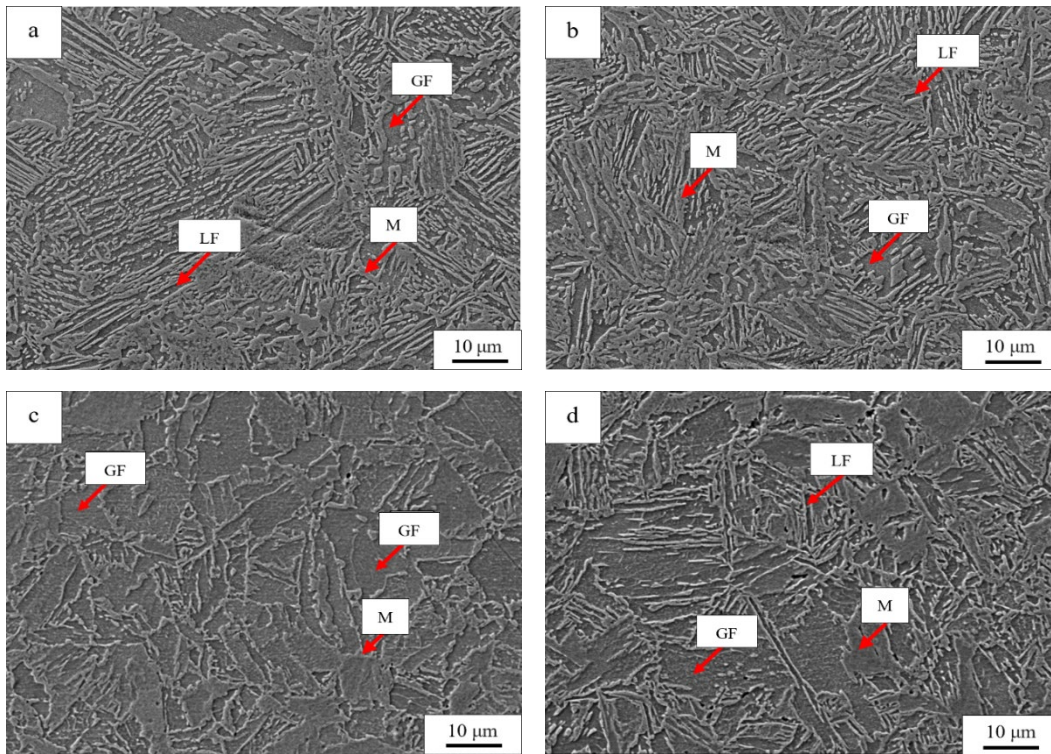


Figure 5. SEM micrographs of (a,b) AC730DIA and (c,d) WQ730DIA [6], (a,c) near surface area and (b,d) at center area. LF: Lath ferrite, GF: Granular ferrite, M: Martensite.

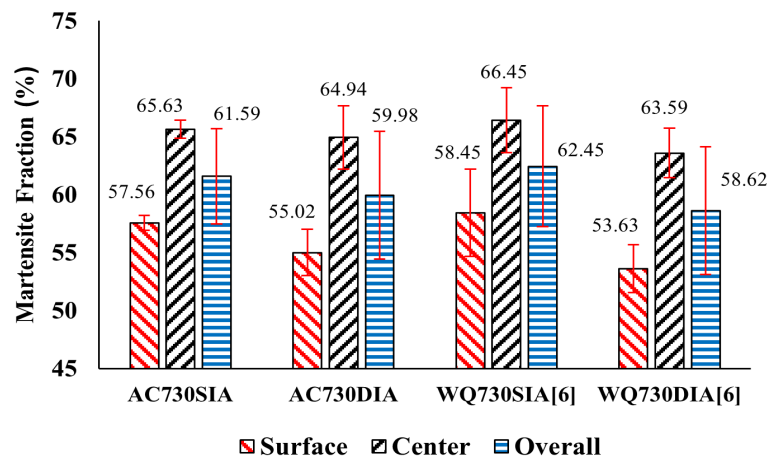


Figure 6. Martensite fraction of the specimens with various heat treatment conditions.

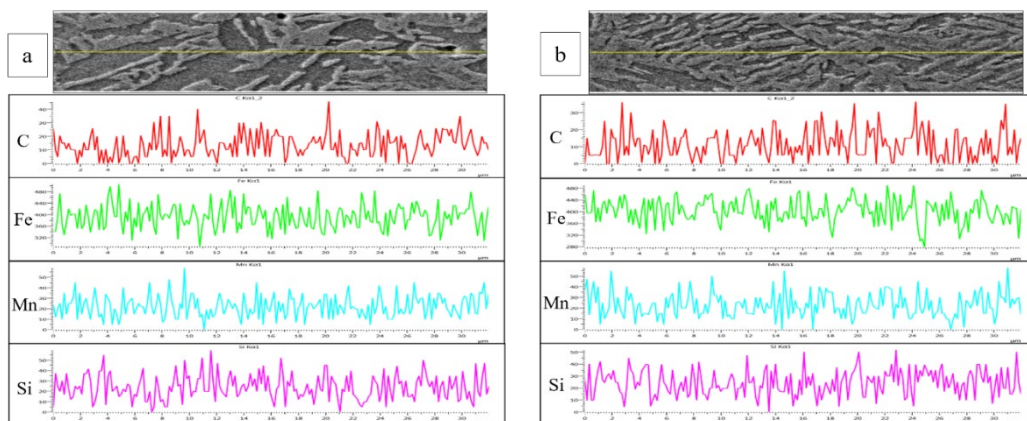


Figure 7. SEM images and EDS line scans of the central area of the (a) AC730SIA, and (b) AC730DIA specimens.

The SEM images and EDS line scan results of AC730SIA and AC730DIA (Figure 7) reveal an absence of distinct cluster of alloying elements, such as manganese and silicon. Conversely, some fluctuations were found in the carbon profile. This is because the holding time is short which allows only that which has a small atomic size can diffuse more easily compared to large elements [25]. The result of AC method of AC method is consistent with WQ method studied before [6].

3.2 Mechanical properties

The engineering stress-strain curves of all specimens are shown in Figure 8, and various average values are presented in Table 4. WQ950 specimens with a martensitic structure, show high strength and low ductility, in contrast to AC950 specimens with a bainitic structure which exhibit lower strength and higher ductility than WQ950 specimens. This demonstrates that mechanical properties were altered by changing the quenching method.

After SIA, both yield and tensile strengths decrease, and ductility increases for both WQ and AC methods. However, WQ730SIA experienced a larger change in the mechanical properties compared to AC730SIA. Moreover, WQ730SIA has higher yield and tensile strengths than that of AC730SIA likely due to the higher martensite content in WQ730SIA specimens. On the other hand, AC730SIA specimen has higher ductility compared to WQ730SIA specimen.

After DIA, both WQ730DIA and AC730DIA experienced a decrease in yield strength and an increase ductility (Table 4). However, AC730DIA has an increase in tensile strength from 659 to 676 MPa. When comparing two conditions, WQ730DIA exhibit DP steels in this work exhibit a little higher strength and ductility than AC730DIA. Nonetheless, this proves that the mechanical properties

of DP steel can be adjusted through double intercritical annealing process. In this work, annealed DP steel exhibits yield strength ranging from 450 MPa to 500 MPa, tensile strength from 675 MPa to 750 MPa, and elongation percentages from 16 to 22%, which are related to the amount of martensite. Generally, increasing martensite content leads to higher tensile strength and yield strength but reduced ductility [5,26]. According to the results, the mechanical property was adjusted to increase the ductility without sacrificing much strength using DIA method.

Additionally, the engineering stress-strain curves shown in Figure 8. reveal that after SIA, the disappearance of the yield point phenomenon and enhancement of the work hardenability are evident. The continuous strain-hardening behavior of DP steel can be explained by the fact that martensite formed after intercritical annealing, generates unpinned dislocations in ferrite (due to shear and volume changes associated with the transformation) [27,28]. These martensite-induced dislocations move at low stress regions, creating low yield strengths, and interact to produce high rates of strain hardening [11].

Furthermore, the amount of strain hardening (seen from the UTS–YS value in Table 4) of AC730SIA, AC730DIA, WQ730SIA, and WQ730DIA specimens are relatively similar. The strain hardening curves in Figure 9 reveal that for SIA and DIA during the plastic deformation region, strain hardening rapidly decreases at low stress and then decreases gradually. Afterward, it will maintain a positive value until necking. However, strain hardening value remains positive for longer in DIA specimens in both WQ and AC conditions. Furthermore, the strain hardening value for WQ730SIA and WQ730DIA specimens are similar to that of AC730SIA and AC730DIA specimens. As for the uniform elongation, AC730SIA and AC730DIA specimens are only slightly different while it is significantly increased in WQ730DIA compared to WQ730SIA.

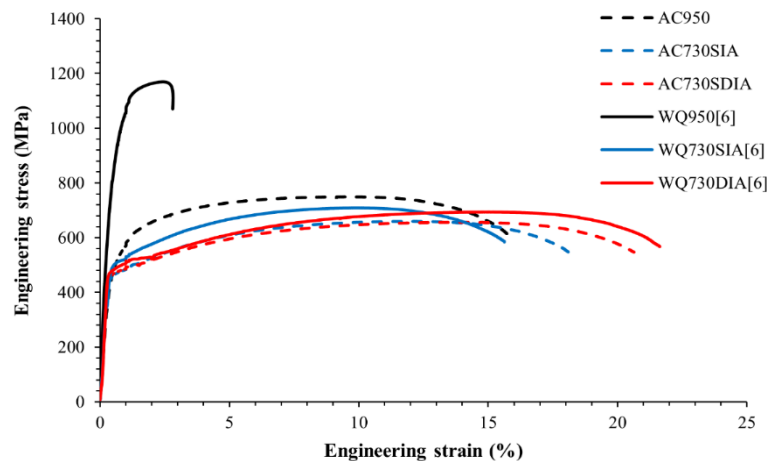


Figure 8. Engineering stress-strain curve of tensile specimens with various heat treatment conditions.

Table 4. Yield strength, tensile strength, elongation, and ultimate elongation of specimens subjected to various heat treatment methods.

Specimen	Yield strength [MPa]	Tensile strength [MPa]	UTS-YS [MPa]	Uniform elongation [%]	Elongation at failure [%]
AC950	463 ± 15	756 ± 5	293	10.5 ± 0.4	15.9 ± 1.6
AC730SIA	459 ± 9	659 ± 1	201	13.3 ± 0.3	19.0 ± 1.1
AC730DIA	449 ± 20	676 ± 19	227	14.1 ± 1.3	20.5 ± 1.7
WQ950[6]	898 ± 8	1164 ± 9	266	2.8 ± 0.4	4.0 ± 1.2
WQ730SIA[6]	504 ± 10	704 ± 4	200	10.4 ± 0.5	16.6 ± 0.8
WQ730DIA[6]	479 ± 3	696 ± 3	217	14.4 ± 0.5	22.0 ± 0.8

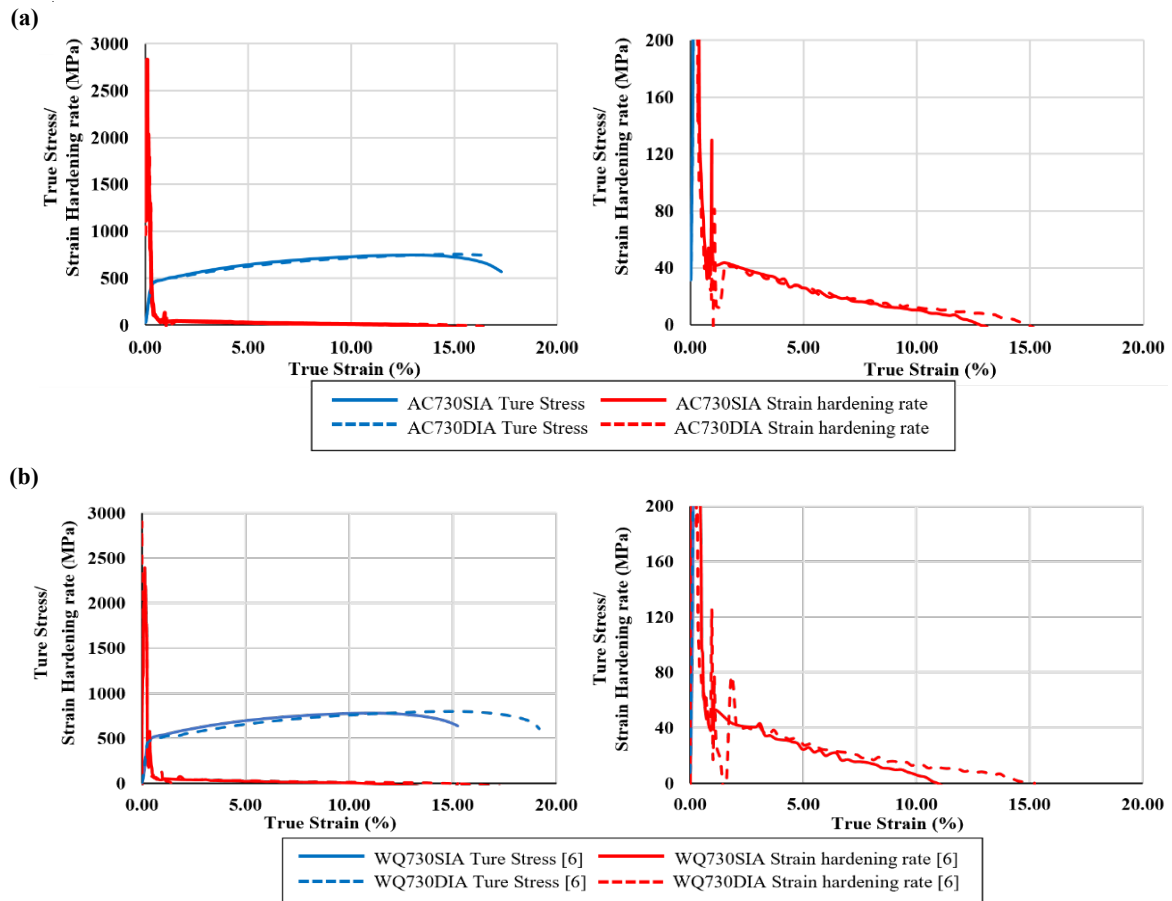


Figure 9. True stress-strain and work hardening curves of (a) AC730SIA and AC730DIA, and (b) WQ730SIA and WQ730DIA specimens intercritical annealed.

3.3 Relationship between microstructure and mechanical properties

According to the obtained microstructure and mechanical properties, all connections were considered. Before intercritical annealing, the WQ method has a high cooling rate resulting in a martensitic structure (Figure 3(c,d)) with high strength but low ductility. Conversely, the AC method has a moderate cooling rate resulting in a bainitic structure (Figure 3(a,b)) leads to lower strength but higher ductility than the WQ method. From other research, it was found that the water quenching method (WQ950) has a higher stress concentration than the air cooling method (AC950) [1].

During SIA, recovery and recrystallization occur, causing the reduction of stress concentration in the workpiece [20]. After water quenching, both AC730SIA and WQ730SIA contain martensite and ferrite in the microstructure. As martensite has a much higher strength than ferrite, the increases in martensite content cause the yield stress and tensile strength to increase, while ductility decreases [27,29,30]. Moreover, a smaller ferrite grain area also results in higher yield stress and tensile strength compared to a larger ferrite grain area [2,27] but the larger ferrite grain area is more ductility [10,18]. In addition, the AC730SIA had less mechanical properties change than the WQ730SIA, both in strength and ductility (See Table 4, Figure 8). This is due to WQ730SIA has higher stress concentration than AC730SIA, leading to earlier recrystallization. Consequently, WQ730SIA has higher martensite

content and a larger ferrite grain area than AC730SIA. In addition, different stress concentrations have different effects on martensite morphology. WQ730SIA exhibits thin and sharp needle dispersed irregularly martensite throughout the microstructure leading to a higher stress concentration. On the other hand, AC730SIA has short and rounded martensite dispersed regularly in a ferrite matrix.

After DIA, recrystallization occurs again resulting in further grain refinement which can increase strength along with improving ductility concurrently [31]. This was evident as a slight reduction in ferrite grain area. However, the microstructure still resembles that of the workpieces that underwent SIA, but with greater homogeneity and lower martensite content. This is consistent with lower yield stress and increased ductility of DIA specimens compared to SIA specimens. Generally, a decrease in martensite content and an increase in ferrite grain area lead to a decrease in both strength and ductility. However, WQ730DIA, with larger ferrite grain area and higher martensite content than AC730DIA (see Table 3, Figure 6), exhibits higher tensile strength and ductility after tensile test. This is because WQ730DIA still has higher stress concentrations than AC730DIA due to the initial martensite structure from austenitizing structure.

The significant feature of the microstructure of WQ730SIA and AC730SIA and WQ730DIA and AC730DIA (Figure 4-5) are large ferrite grain area (Table 3) and low martensite content (Figure 6) near surface compared to center of the workpiece. It found that WQ730SIA has the most inhomogeneous microstructure due to the

rapid recrystallization caused by high stress concentration. After DIA, WQ730DIA has a more uniform distribution, making the microstructure more homogeneous. In the case of the AC method the microstructure more uniform because the lower stress concentration leads to less transformation.

Additionally, for mechanical properties, an increase in the amount ferrite grain areas leads to increased ductility [29,30] and slightly decreasing the ferrite grain area has a beneficial effect on strength and ductility [1]. Moreover, the decrease in martensite content leads to an increase in carbon content in the martensite and a reduction in the strain-hardening exponent of DP steel [32]. Also the increased number of granular ferrite in the center area after DIA, compared to the predominantly lath ferrite found in SIA specimens, is beneficial for strain hardening behavior. Thus, the strain hardening during plastic deformation sustains a positive value to a larger true strain (Figure 9).

Furthermore, some studies [4,5] have revealed that grain refinement in DP steel differs from other metal materials. Grain refinement normally leads to a decrease in the initial strain hardening rate, increasing yield stress and slightly tensile strength and decreasing ductility [27]. However, this does not apply to DP steel due to the presence of martensite fibers that increase ductility [13]. DP steel when undergoes deformation, stress concentrations occur in the ferrite which has low strength. Plastic strain in ferrite is constrained by adjacent martensite grains, resulting in an accumulated strain near the interface boundaries of ferrite and martensite [33].

3.4 Comparison between cooling methods (water quenching and air cooling) after austenitizing

After austenitized, water quenching produces a higher cooling rate than air cooling. Thus, WQ950 specimens has fully martensite structure which has higher stress concentrations than bainitic structure in AC950. After the first intercritical annealing, WQ950 undergoes a phase transformation to austenite and ferrite during intercritical annealing earlier than AC950. This is because the martensitic structure in WQ950 structure, does not need to dissolve carbides, whereas the bainitic structure does. For these two reasons, WQ730SIA recrystallized before AC730SIA. This is consistent with the microstructure that WQ730SIA contains thin and sharp needle martensite dispersed irregularly in matrix with a higher stress concentration compared to short and rounded martensite in AC730SIA. It was also observed that WQ730SIA specimen has larger ferrite grain area and martensite fraction than AC730SIA, while AC730SIA specimen shows more homogeneous structure, which relates to the effect of elier grain growth in WQ730SIA compared to AC730SIA.

After intercritical annealing for second time, specimes underwent repeated recrystallization, the concentration stress decreased, leading to a reduction in the ferrite grain area. The microstructure characteristics remained similar to the previous structure after the first intercritical annealing, but are more homogeneous in both workpieces. However, the recrystallization throughout the entire area was incomplete due to insufficient energy, as the annealing temperature was low. Although the stress concentration decreased, the WQ730DIA workpiece still has higher stress concentration than the AC730SIA. This is because WQ730DIA has a greater difference in the martensite fraction near surface area compared to center area than AC730DIA. Therefore,

the AC730DIA workpiece had more uniform microstructure than WQ730DIA.

In term of mechanical properties, AC730SIA specimen has lower strength but higher ductility than WQ730SIA specimen, because of the lower stress concentration and martensite fraction. After double intercritical annealing, WQ730DIA shows higher yield strength and tensile strength than AC730DIA, with similar ductility. From further investigation, it was found that in addition to stress concentration, water quenching produces higher residual stress than air cooling [20,34]. However, the mechanical properties values are not much different between two methods even though the WQ method specimens have higher stress concentrations and residual stress.

Results from the mechanical testing of 0.11%C-2.39%Mn-0.45%Si dual phase steel subjected to double intercritical annealing at 730°C show yield stress of 450 MPa to 500 MPa, tensile strength of 675 MPa to 750 MPa and elongation of 16% to 22%. This study confirmed that DIA can modify and enhance the mechanical properties of DP steel. WQ method provides slightly higher strength and ductility compared to AC method. However, water quenching from high temperature after austenitizing poses a risk of cracks in larger-sized workpieces and distortion in smaller-sized ones, making air cooling a preferable option after austenitizing.

4. Conclusions

In this article, 0.107%C-2.39%Mn-0.453%Si dual-phase steel was subjected to the DIA process at 730°C. The effects of water quenching and air cooling methods after austenitizing on the microstructure and mechanical properties after DIA were studied. The significant results can be observed as follows.

1. After SIA, WQ specimens recrystallization before AC specimens, resulting in larger martensite quantities and ferrite grain areas compared to AC method. Therefore, WQ method exhibit higher strengths, but AC method had greater ductility.
2. After DIA, recrystallization results in further grain refinement. The ferrite grain areas and martensite content slightly decrease for both WQ and AC methods. The WQ method exhibits higher strengths and ductility compared to AC method because WQ has a higher stress concentration than AC. Since both have similar amounts of martensite content and ferrite grain area, they cause little effect on the difference in mechanical properties.
3. After DIA, the ferrite grain area decreased, and martensite became more homogeneous and distributed throughout the specimens which benefitted the strain hardening behavior during plastic deformation, increasing the homogeneity of the microstructure and enhancing ductility.
4. DIA leads to changes in the mechanical properties of DP steel and has the potential to improve them. However, appropriate values such as holding time, holding temperature, and heating and cooling rates should be further investigated to optimize the effectiveness of this method.
5. Although the WQ method has higher yield stress, tensile strength and ductility than the AC method. The risk of the workpiece bending, warping, or cracking during the quenching process after austenitizing outweighed the benefits. Therefore, the AC method is a better option. Since the mechanical properties are only slightly less than the WQ method.

References

- [1] M. Tisza, "Three Generations of advanced high strength steels in the automotive industry," in the *Vehicle and Automotive Engineering 3: Proceedings of the 3rd VAE2020, Miskolc, Hungary*, 2020, pp. 81-94.
- [2] F. Najafkhani, H. Mirzadeh, and M. Zamani, "Effect of intercritical annealing conditions on grain growth kinetics of dual phase steel," *Metals and Materials International*, vol. 25, pp. 1039-1046, 2019.
- [3] D. Cooman, "Fundamentals of steel product physical metallurgy," *Association for Iron & Steel Technology*, 2011.
- [4] S. Ghaemifar, and H. Mirzadeh, "Refinement of banded structure via thermal cycling and its effects on mechanical properties of dual phase steel," *Steel Research International*, vol. 89, no. 6, p. 1700531, 2018.
- [5] C. Zheng and D. Raabe, "Interaction between recrystallization and phase transformation during intercritical annealing in a cold-rolled dual-phase steel: A cellular automaton model," *Acta Materialia*, vol. 61, no. 14, pp. 5504-5517, 2013.
- [6] N. Saenarjhan, G. Lothongkum, and J. Opapaiboon, "The effects of double intercritical annealing on microstructure and mechanical properties of 0.107 C-2.39 Mn-0.453 Si dual phase steel," *Journal of Metals, Materials and Minerals*, vol. 32, no. 4, pp. 109-117, 2022.
- [7] H. K. Zeytin, C. Kubilay, and H. Aydin, "Investigation of dual phase transformation of commercial low alloy steels: Effect of holding time at low inter-critical annealing temperatures," *Materials Letters*, vol. 62, no. 17-18, pp. 2651-2653, 2008.
- [8] P. Movahed, S. Kolahgar, S. Marashi, M. Pouranvari, and N. Parvin, "The effect of intercritical heat treatment temperature on the tensile properties and work hardening behavior of ferrite-martensite dual phase steel sheets," *Materials Science and Engineering: A*, vol. 518, no. 1-2, pp. 1-6, 2009.
- [9] A. Kalhor, and H. Mirzadeh, "Tailoring the microstructure and mechanical properties of dual phase steel based on the initial microstructure," *Steel Research International*, vol. 88, no. 8, p. 1600385, 2017.
- [10] M. Sudo, and I. Kokubo, "Microstructure-mechanical property relationships in multi-phase steel sheet," *Scandinavian journal of metallurgy*, vol. 13, no. 6, pp. 329-342, 1984.
- [11] M. Maleki, H. Mirzadeh, and M. Zamani, "Effect of intercritical annealing on mechanical properties and work-hardening response of high formability dual phase steel," *Steel Research International*, vol. 89, p. 1700412, 2018.
- [12] L. H. Wang, D. Tang, H. T. Jiang, J. B. Liu, and Y. Chen, "Effects of continuous annealing process on microstructures and properties of C-Mn-Si bearing cold-rolled trip steel," *Advanced Materials Research*, vol. 602, pp. 472-477, 2013.
- [13] K. Park, M. Nishiyama, N. Nakada, T. Tsuchiyama, and S. Takaki, "Effect of the martensite distribution on the strain hardening and ductile fracture behaviors in dual-phase steel," *Materials Science and Engineering: A*, vol. 604, pp. 135-141, 2014.
- [14] H. Dong, and X. Sun, "Deformation induced ferrite transformation in low carbon steels," *Current Opinion in Solid State and Materials Science*, vol. 9, no. 6, pp. 269-276, 2005.
- [15] M.-h. Park, A. Shibata, and N. Tsuji, "Effect of grain size on mechanical properties of dual phase steels composed of ferrite and martensite," *MRS Advances*, vol. 1, pp. 1-6, 2016.
- [16] A. A. Gorni, "Steel forming and heat treating handbook," *São Vicente, Brazil*, vol. 24, 2011.
- [17] V. D. Eisenhüttenleute, *Steel-A Handbook for materials research and engineering: Volume 1: Fundamentals*. Springer, 1992.
- [18] D. Sun, Z. Guo, and J. Gu, "The microstructure and crystallography of lath martensite with Greninger-Troiano orientation relationship in a Fe-12.8 Ni-1.5 Si-0.22% C steel," *Materials Characterization*, vol. 181, p. 111501, 2021.
- [19] C. Wang, X. Wang, J. Kang, G. Yuan, and G. Wang, "Effect of thermomechanical treatment on acicular ferrite formation in Ti-Ca deoxidized low carbon steel," *Metals*, vol. 9, no. 3, p. 296, 2019.
- [20] A. Samuel, and K. N. Prabhu, "Residual stress and distortion during quench hardening of steels: A review," *Journal of Materials Engineering and Performance*, vol. 31, no. 7, pp. 5161-5188, 2022.
- [21] F. Najafkhani, H. Mirzadeh, and M. Zamani, "Effect of intercritical annealing conditions on grain growth kinetics of dual phase steel," *Metals and Materials International*, vol. 25, 2019.
- [22] C. Tasan, M. Diehl, D. Yan, M. Bechtold, F. Roters, L. Schemmann, C. Zheng, N. Peranio, D. Ponge, M. P. Koyama, K. Tsuzaki, and D. Raabe, "An overview of dual-phase steels: advances in microstructure-oriented processing and micromechanically guided design," *Annual Review of Materials Research*, vol. 45, pp. 391-431, 2015.
- [23] C. Bos, M. Mecozzi, and J. Sietsma, "A microstructure model for recrystallisation and phase transformation during the dual-phase steel annealing cycle," *Computational Materials Science*, vol. 48, no. 3, pp. 692-699, 2010.
- [24] N. Peranio, Y. Li, F. Roters, and D. Raabe, "Microstructure and texture evolution in dual-phase steels: Competition between recovery, recrystallization, and phase transformation," *Materials Science and Engineering: A*, vol. 527, no. 16-17, pp. 4161-4168, 2010.
- [25] L. Schemmann, S. Zaeferrer, D. Raabe, F. Friedel, and D. Mattissen, "Alloying effects on microstructure formation of dual phase steels," *Acta Materialia*, vol. 95, pp. 386-398, 2015.
- [26] E. Aşık, E. Perdahcıoğlu, and A. van den Boogaard, "Microscopic investigation of damage mechanisms and anisotropic evolution of damage in DP600," *Materials Science and Engineering: A*, vol. 739, pp. 348-356, 2019.
- [27] M. Calcagnotto, D. Ponge, E. Demir, and D. Raabe, "Orientation gradients and geometrically necessary dislocations in ultrafine grained dual-phase steels studied by 2D and 3D EBSD," *Materials Science and Engineering: A*, vol. 527, no. 10-11, pp. 2738-2746, 2010.
- [28] G. Krauss, "*Steels: processing, structure, and performance*," ASM International, 2015.

- [29] N. Nakada, Y. Arakawa, K.-S. Park, T. Tsuchiyama, and S. Takaki, "Dual phase structure formed by partial reversion of cold-deformed martensite," *Materials Science and Engineering: A*, vol. 553, pp. 128-133, 2012.
- [30] S. Nikkhah, H. Mirzadeh, and M. Zamani, "Fine tuning the mechanical properties of dual phase steel via thermomechanical processing of cold rolling and intercritical annealing," *Materials Chemistry and Physics*, vol. 230, pp. 1-8, 2019.
- [31] M. Calcagnotto, Y. Adachi, D. Ponge, and D. Raabe, "Deformation and fracture mechanisms in fine-and ultrafine-grained ferrite/ martensite dual-phase steels and the effect of aging," *Acta Materialia*, vol. 59, no. 2, pp. 658-670, 2011.
- [32] A. H. Jahanara, Y. Mazaheri, and M. Sheikhi, "Correlation of ferrite and martensite micromechanical behavior with mechanical properties of ultrafine grained dual phase steels," *Materials Science and Engineering: A*, vol. 764, p. 138206, 2019.
- [33] M. Balbi, I. Alvarez-Armas, and A. Armas, "Effect of holding time at an intercritical temperature on the microstructure and tensile properties of a ferrite-martensite dual phase steel," *Materials Science and Engineering: A*, vol. 733, pp. 1-8, 2018.
- [34] N. Peranio, F. Roters, and D. Raabe, "Microstructure evolution during recrystallization of dual-phase steels," *Materials Science Forum*, vol. 715-716, p. 13-22, 2012.